Mathematical analysis of ultrafast ultrasound imaging

Giovanni S Alberti

Department of Mathematics, University of Genoa

Joint work with H. Ammari (ETH), F. Romero (ETH) and T. Wintz (ENS).

AIPC 2017, May 30

From ultrasonography to ultrafast ultrasonography

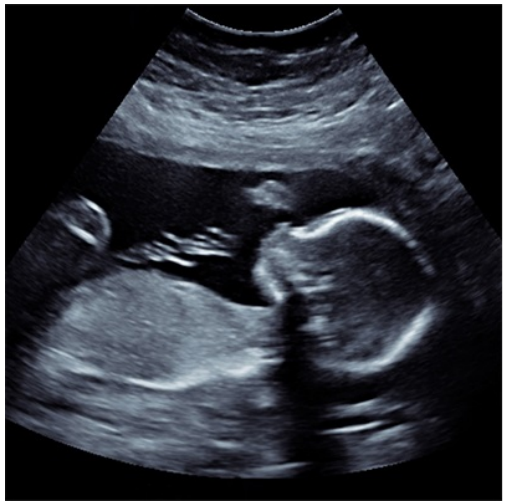

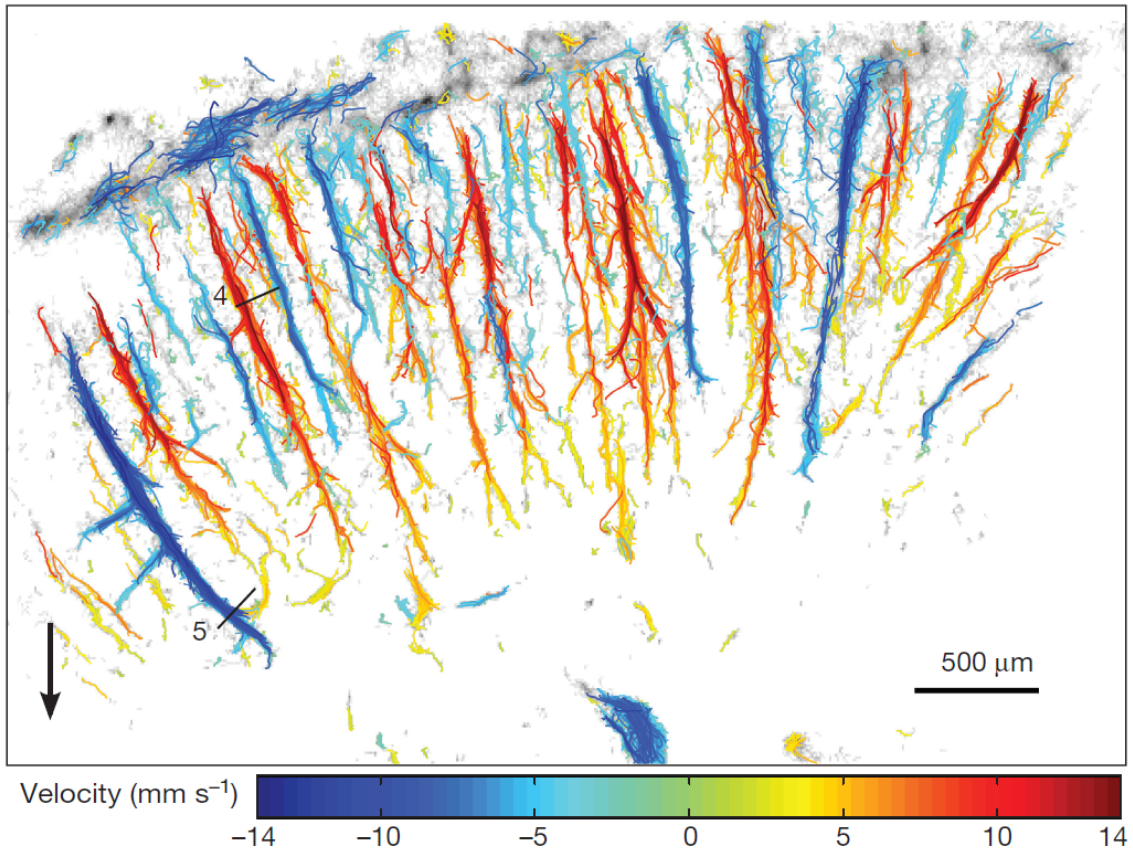

Errico et. al, Nature 527, 499–502, 2015

Conventional ultrasonography

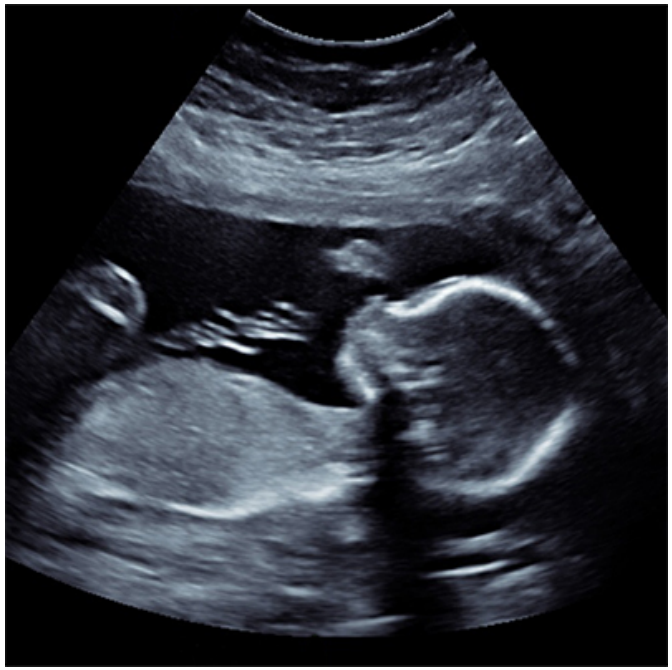

Conventional ultrasound imaging:

- focused ultrasonic waves
- high spatial resolution
- long acquisition time
- very low contrast: soft biological tissues are almost acoustically homogeneous, due to the high water concentration
- fine details (such as blood vessels) are completely invisible

Ultrafast ultrasound imaging

- Use of plane waves instead of focused waves
- High frame rate: up to 20,000 frames per second
- Lots of data to post-process: we focus on blood flow imaging

Demené et al., IEEE Trans Med Imaging, 2015.

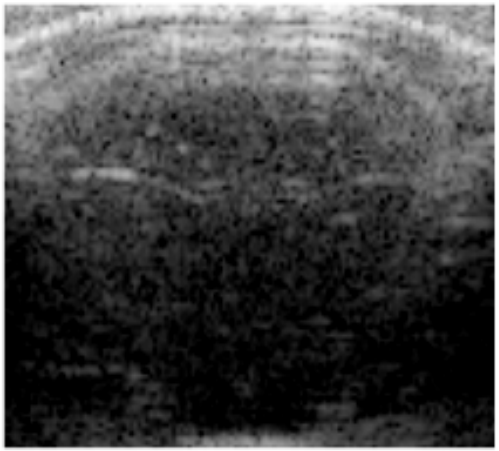

Single frame of Ultrafast ultrasound brain of a thinned skull rat

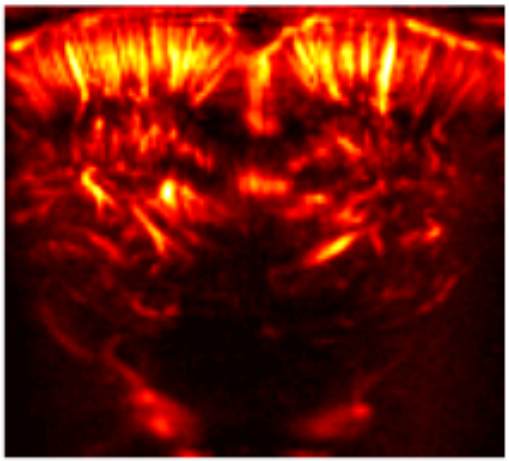

Power doppler image obtained via a SVD filter applied to 250 frames.

Errico et. al, Nature, 2015

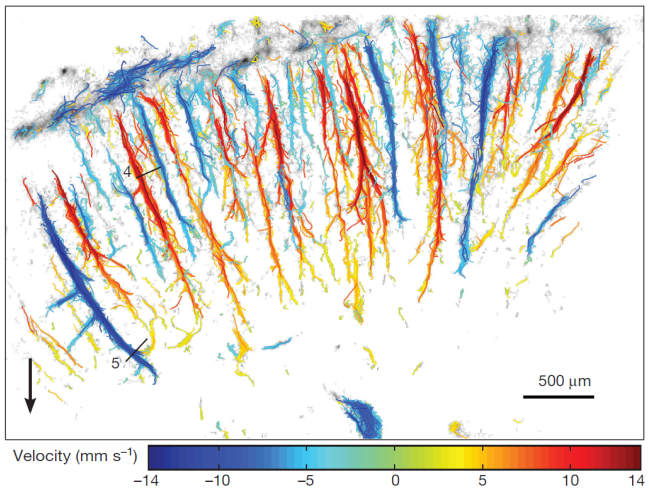

Superresolution: 75,000 frames with blinking microbubbles

Blood flow imaging

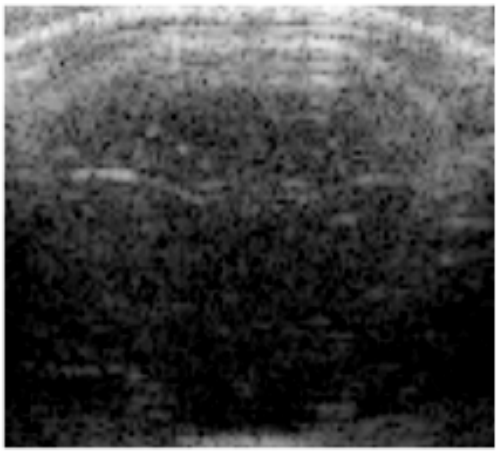

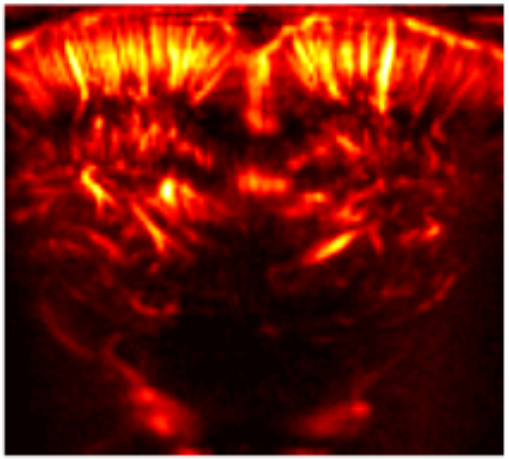

- The main issue is the removal of the clutter signal (the scattering coming from the tissue)
- Ultrafast ultrasonography allows us to overcome this issue, thanks to the very high frame rate.
- Idea: blood moves, tissue does not (in general).
- Temporal filters (Bercoff et al., 2011): high-pass filtering the data to remove clutter signals. Drawback: not applicable when the clutter and blood velocities are close.
- Idea: tissue movement is spatially coherent, while blood flow is not.
- Spatiotemporal method based on the SVD of the data (Demene et al., 2015): exploits the different spatial coherence of the clutter and blood scatterers.

Blood flow imaging

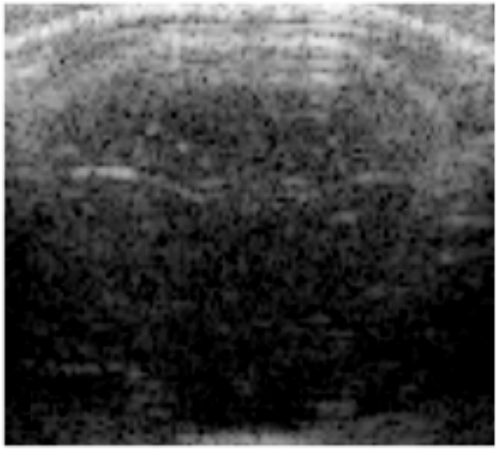

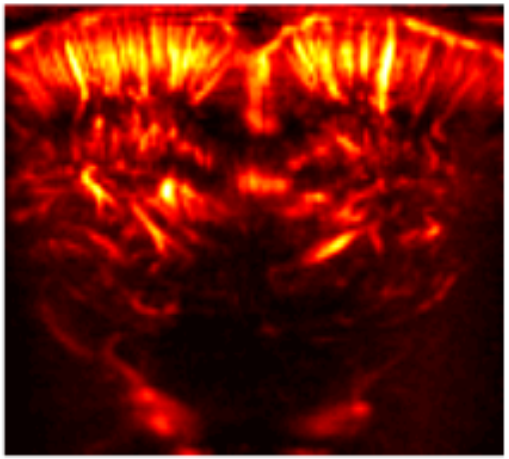

- The main issue is the removal of the clutter signal (the scattering coming from the tissue)
- Ultrafast ultrasonography allows us to overcome this issue, thanks to the very high frame rate.
- Idea: blood moves, tissue does not (in general).
- Temporal filters (Bercoff et al., 2011): high-pass filtering the data to remove clutter signals. Drawback: not applicable when the clutter and blood velocities are close.
- Idea: tissue movement is spatially coherent, while blood flow is not.
- Spatiotemporal method based on the SVD of the data (Demene et al., 2015): exploits the different spatial coherence of the clutter and blood scatterers.

Blood flow imaging

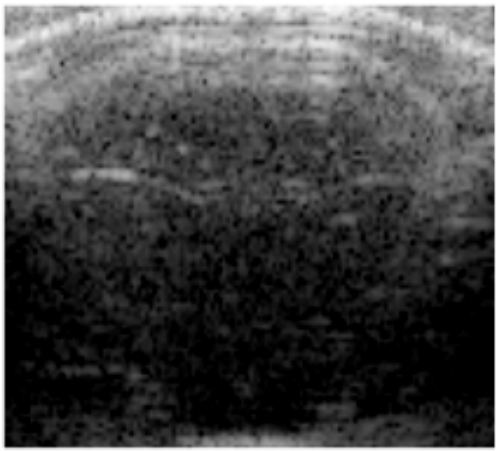

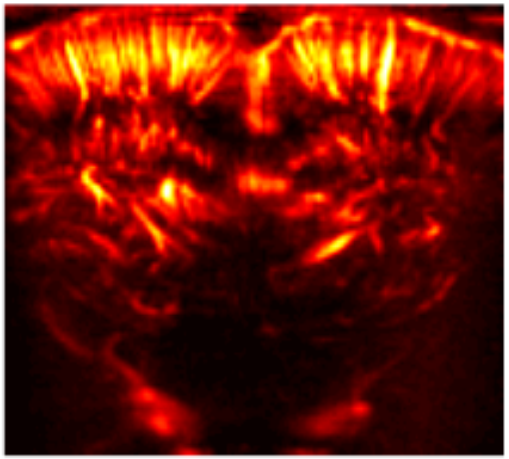

- The main issue is the removal of the clutter signal (the scattering coming from the tissue)
- Ultrafast ultrasonography allows us to overcome this issue, thanks to the very high frame rate.
- Idea: blood moves, tissue does not (in general).
- Temporal filters (Bercoff et al., 2011): high-pass filtering the data to remove clutter signals. Drawback: not applicable when the clutter and blood velocities are close.
- Idea: tissue movement is spatially coherent, while blood flow is not.
- Spatiotemporal method based on the SVD of the data (Demene et al., 2015): exploits the different spatial coherence of the clutter and blood scatterers.

The static direct problem

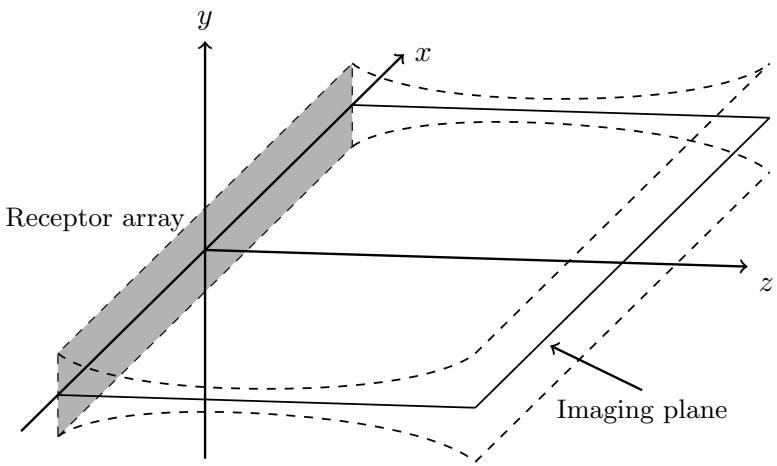

The imaging system

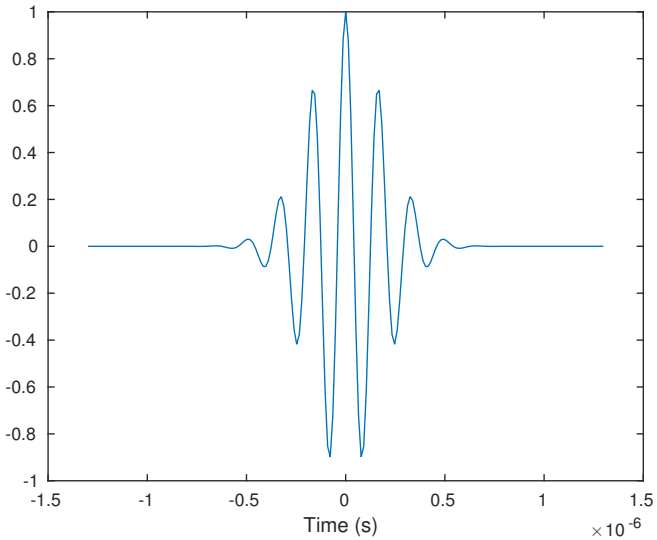

The pulse $f(t) = e^{2\pi i \nu_0 t} \chi(\nu_0 t)$

- Incident field in the direction $\mathbf{k}_\theta = (\sin\theta, \cos\theta)$:

$$u^i(x, y, z, t) = A_z(y) f\left(t - c_0^{-1} \mathbf{k}_\theta \cdot (x, z)\right)$$

- c_0 : background speed of sound. $c(\mathbf{x})$: speed of sound. Perturbation:

$$n(\mathbf{x}) = \frac{1}{c^2(\mathbf{x})} - \frac{1}{c_0^2}$$

- In the Born approximation, the scattered field takes the form:

$$u^s(\mathbf{u}_0, t) = -\int_{\mathbb{R}^2} \frac{(4\pi)^{-1}}{|\mathbf{u}_0 - \mathbf{x}'|} f''\left(t - \frac{\mathbf{x}' \cdot \mathbf{k}_\theta + |\mathbf{u}_0 - \mathbf{x}'|}{c_0}\right) n(\mathbf{x}')\, d\mathbf{x}', \quad \mathbf{u}_0 = (u, 0)$$

The static direct problem

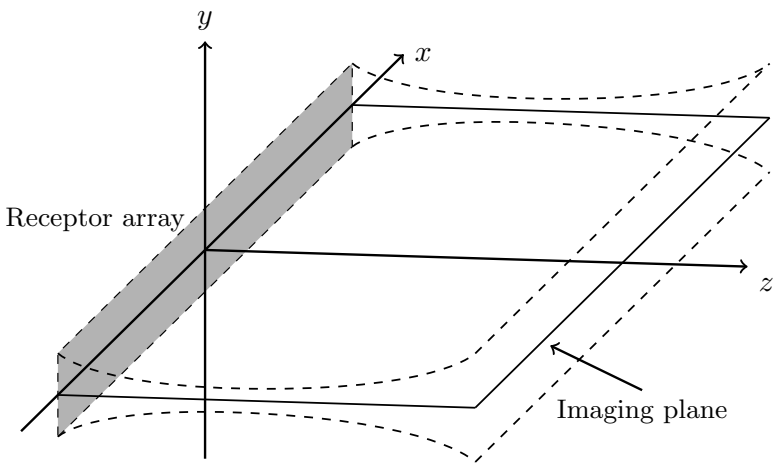

The imaging system

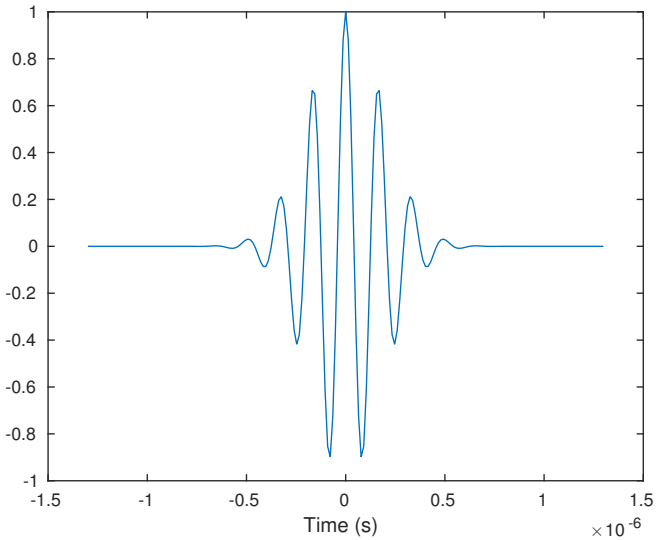

The pulse $f(t) = e^{2\pi i \nu_0 t} \chi(\nu_0 t)$

- Incident field in the direction $\mathbf{k}_\theta = (\sin\theta, \cos\theta)$:

$$u^i(x, y, z, t) = A_z(y) f\left(t - c_0^{-1} \mathbf{k}_\theta \cdot (x, z)\right)$$

- c_0 : background speed of sound. $c(\mathbf{x})$: speed of sound. Perturbation:

$$n(\mathbf{x}) = \frac{1}{c^2(\mathbf{x})} - \frac{1}{c_0^2}$$

- In the Born approximation, the scattered field takes the form:

$$u^s(\mathbf{u}_0, t) = -\int_{\mathbb{R}^2} \frac{(4\pi)^{-1}}{|\mathbf{u}_0 - \mathbf{x}'|} f''\left(t - \frac{\mathbf{x}' \cdot \mathbf{k}_\theta + |\mathbf{u}_0 - \mathbf{x}'|}{c_0}\right) n(\mathbf{x}')\, d\mathbf{x}', \quad \mathbf{u}_0 = (u, 0)$$

The static direct problem

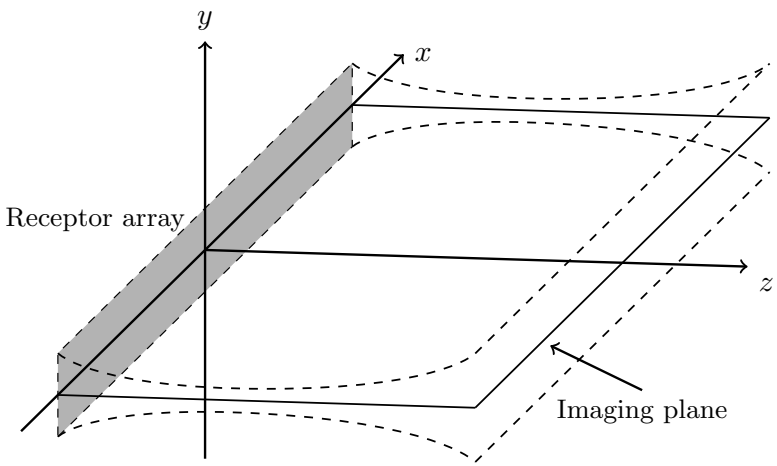

The imaging system

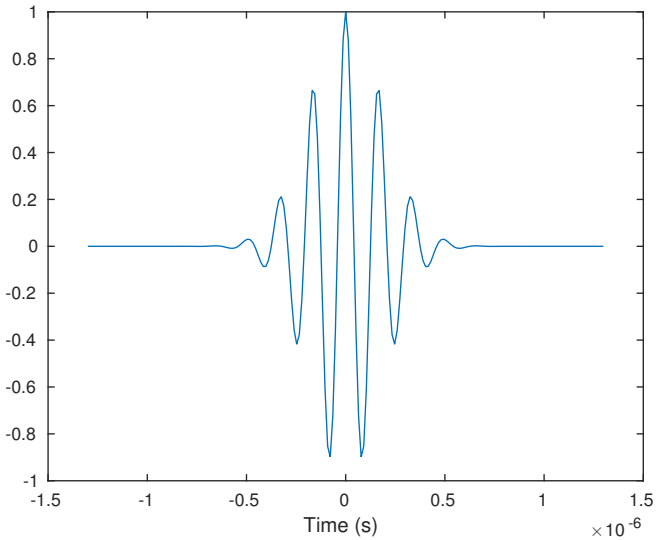

The pulse $f(t) = e^{2\pi i \nu_0 t} \chi(\nu_0 t)$

- Incident field in the direction $\mathbf{k}_\theta = (\sin\theta, \cos\theta)$:

$$u^i(x, y, z, t) = A_z(y) f\left(t - c_0^{-1} \mathbf{k}_\theta \cdot (x, z)\right)$$

- c_0 : background speed of sound. $c(\mathbf{x})$: speed of sound. Perturbation:

$$n(\mathbf{x}) = \frac{1}{c^2(\mathbf{x})} - \frac{1}{c_0^2}$$

- In the Born approximation, the scattered field takes the form:

$$u^s(\mathbf{u}_0, t) = -\int_{\mathbb{R}^2} \frac{(4\pi)^{-1}}{|\mathbf{u}_0 - \mathbf{x}'|} f''\left(t - \frac{\mathbf{x}' \cdot \mathbf{k}_\theta + |\mathbf{u}_0 - \mathbf{x}'|}{c_0}\right) n(\mathbf{x}')\, d\mathbf{x}', \quad \mathbf{u}_0 = (u, 0)$$

The static inverse problem: beamforming

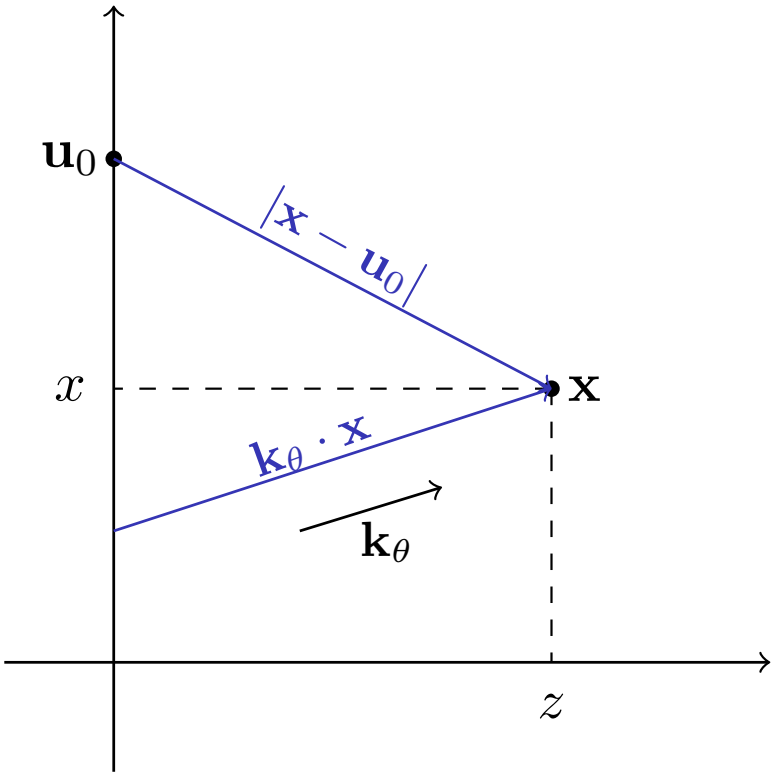

- Scattered field

$$u^s(\mathbf{u}_0, t), \qquad \mathbf{u}_0 = (u, 0),\ t > 0$$

- Travel time from the receptor array Γ to a point $\mathbf{x}$ and back to a receptor in $\mathbf{u}_0$:

$$\tau^\theta_{\mathbf{x}}(u) = c_0^{-1}(\mathbf{k}_\theta \cdot \mathbf{x} + |\mathbf{x} - \mathbf{u}_0|)$$

- Beamforming: averaging the signals

$$s_\theta(x, z) := \int_{x-Fz}^{x+Fz} u^s\left(\mathbf{u}_0, \tau^\theta_{\mathbf{x}}(u)\right) du$$

Inserting the expression for u^s obtained before we obtain

$$s_\theta(\mathbf{x}) = \int_{\mathbf{x}' \in \mathbb{R}^2} n(\mathbf{x}') \underbrace{\int_{x-Fz}^{x+Fz} -\frac{(4\pi)^{-1}}{|\mathbf{x}' - \mathbf{u}_0|} f''\left(\tau^\theta_{\mathbf{x}}(u) - \tau^\theta_{\mathbf{x}'}(u)\right) du}_{=g_\theta(\mathbf{x}, \mathbf{x}')} d\mathbf{x}'$$

The static inverse problem: beamforming

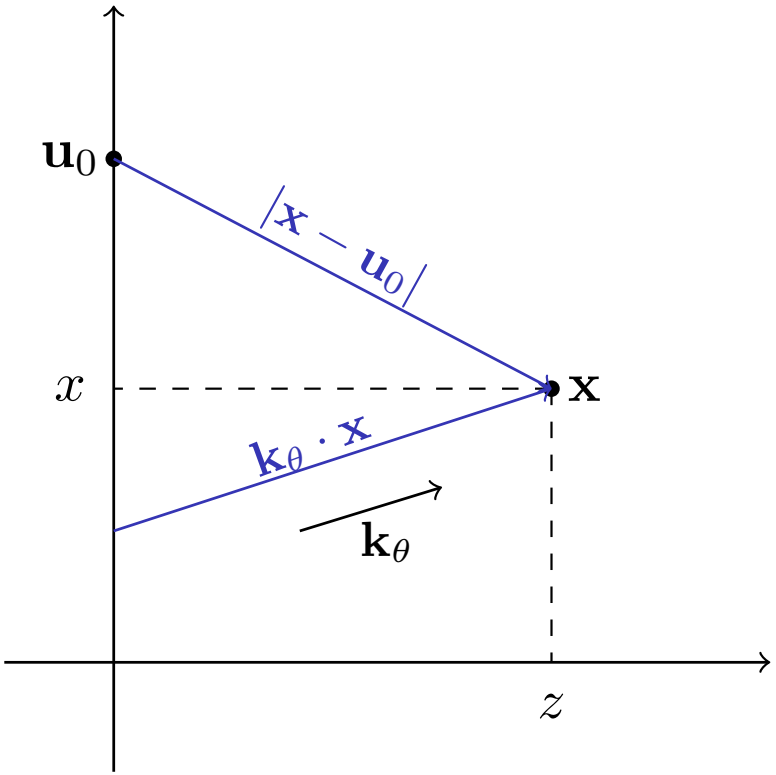

- Scattered field

$$u^s\left(\mathbf{u}_0, t\right), \qquad \mathbf{u}_0 = (u, 0),\ t > 0$$

- Travel time from the receptor array Γ to a point $\mathbf{x}$ and back to a receptor in $\mathbf{u}_0$:

$$\tau_{\mathbf{x}}^{\theta}(u) = c_0^{-1}(\mathbf{k}_\theta \cdot \mathbf{x} + |\mathbf{x} - \mathbf{u}_0|)$$

- Beamforming: averaging the signals

$$s_\theta(x, z) := \int_{x-Fz}^{x+Fz} u^s\left(\mathbf{u}_0, \tau_{\mathbf{x}}^{\theta}\left(u\right)\right) du$$

Inserting the expression for u^s obtained before we obtain

$$s_\theta(\mathbf{x}) = \int_{\mathbf{x}' \in \mathbb{R}^2} n\left(\mathbf{x}'\right) \underbrace{\int_{x-Fz}^{x+Fz} -\frac{(4\pi)^{-1}}{|\mathbf{x}' - \mathbf{u}_0|} f''\left(\tau_{\mathbf{x}}^{\theta}\left(u\right) - \tau_{\mathbf{x}'}^{\theta}\left(u\right)\right) du}_{=g_\theta(\mathbf{x},\mathbf{x}')} d\mathbf{x}'$$

The static inverse problem: beamforming

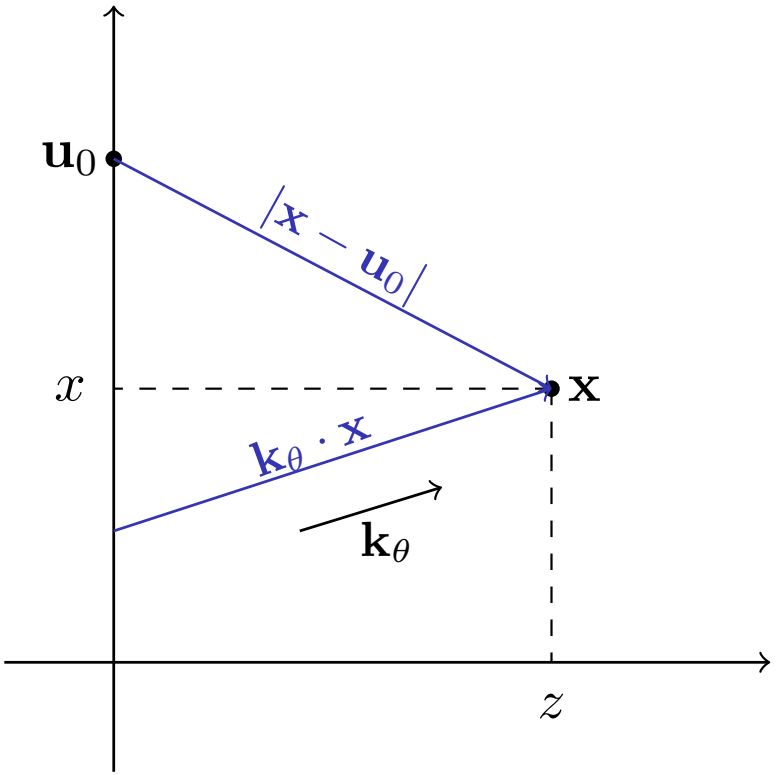

- Scattered field

$$u^s\left(\mathbf{u}_0, t\right), \qquad \mathbf{u}_0 = (u, 0),\ t > 0$$

- Travel time from the receptor array Γ to a point $\mathbf{x}$ and back to a receptor in $\mathbf{u}_0$:

$$\tau_{\mathbf{x}}^{\theta}(u) = c_0^{-1}(\mathbf{k}_\theta \cdot \mathbf{x} + |\mathbf{x} - \mathbf{u}_0|)$$

- Beamforming: averaging the signals

$$s_\theta(x, z) := \int_{x-Fz}^{x+Fz} u^s\left(\mathbf{u}_0, \tau_{\mathbf{x}}^{\theta}\left(u\right)\right) du$$

Inserting the expression for u^s obtained before we obtain

$$s_\theta(\mathbf{x}) = \int_{\mathbf{x}' \in \mathbb{R}^2} n\left(\mathbf{x}'\right) \underbrace{\int_{x-Fz}^{x+Fz} -\frac{(4\pi)^{-1}}{\left|\mathbf{x}' - \mathbf{u}_0\right|} f''\left(\tau_{\mathbf{x}}^{\theta}\left(u\right) - \tau_{\mathbf{x}'}^{\theta}\left(u\right)\right) du}_{=g_\theta(\mathbf{x},\mathbf{x}')} d\mathbf{x}'$$

The static inverse problem: the point spread function

- The static image s_θ may be rewritten as

$$s_\theta(\mathbf{x}) = \int_{\mathbf{x}' \in \mathbb{R}^2} g_\theta\left(\mathbf{x}, \mathbf{x}'\right) n\left(\mathbf{x}'\right) d\mathbf{x}',$$

where g_θ is the point spread function of the system:

$$g_\theta\left(\mathbf{x}, \mathbf{x}'\right) = -\int_{x-Fz}^{x+Fz} \frac{(4\pi)^{-1}}{|\mathbf{x}' - \mathbf{u}_0|} f''\left(\tau_{\mathbf{x}}^\theta(u) - \tau_{\mathbf{x}'}^\theta(u)\right) du$$

- The PSF may be approximated with a convolution

$$g_\theta(\mathbf{x}, \mathbf{x}') \approx \tilde{g}_\theta(\mathbf{x} - \mathbf{x}'), \qquad s_\theta = \tilde{g}_\theta * n,$$

where ($f_0 = \nu_0 c_0^{-1}$ and $\tilde{\chi} = 2\pi i \chi + \chi'$)

$$\tilde{g}_\theta(\mathbf{x}) \approx -i\nu_0^2 F\, \tilde{\chi}\left(2f_0 z\right) e^{4\pi i f_0 z} e^{2\pi i f_0 \theta x} \operatorname{sinc}(2\pi f_0 F x)$$

The static inverse problem: the point spread function

- The static image s_θ may be rewritten as

$$s_\theta(\mathbf{x}) = \int_{\mathbf{x}' \in \mathbb{R}^2} g_\theta\left(\mathbf{x}, \mathbf{x}'\right) n\left(\mathbf{x}'\right) d\mathbf{x}',$$

where g_θ is the point spread function of the system:

$$g_\theta\left(\mathbf{x}, \mathbf{x}'\right) = -\int_{x-Fz}^{x+Fz} \frac{(4\pi)^{-1}}{|\mathbf{x}' - \mathbf{u}_0|} f''\left(\tau_{\mathbf{x}}^\theta(u) - \tau_{\mathbf{x}'}^\theta(u)\right) du$$

- The PSF may be approximated with a convolution

$$g_\theta(\mathbf{x}, \mathbf{x}') \approx \tilde{g}_\theta(\mathbf{x} - \mathbf{x}'), \qquad s_\theta = \tilde{g}_\theta * n,$$

where ($f_0 = \nu_0 c_0^{-1}$ and $\tilde{\chi} = 2\pi i \chi + \chi'$)

$$\tilde{g}_\theta(\mathbf{x}) \approx -i\nu_0^2 F\, \tilde{\chi}\left(2f_0 z\right) e^{4\pi i f_0 z} e^{2\pi i f_0 \theta x} \operatorname{sinc}(2\pi f_0 F x)$$

The point spread function

In the particular case $\theta = 0$:

$$\tilde{g}_0(\mathbf{x}) \approx -i\nu_0^2 F\, \tilde{\chi}\left(2f_0 z\right)\, e^{4\pi i f_0 z}\, \mathrm{sinc}(2\pi f_0 F x)$$

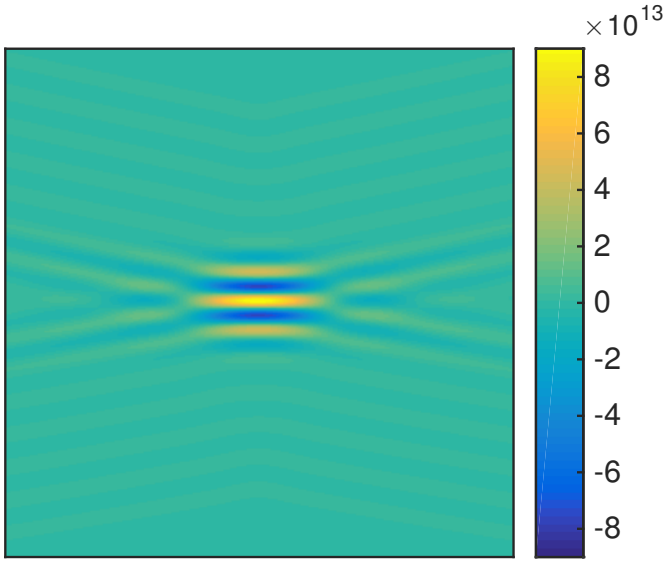

The real part of the PSF g_0

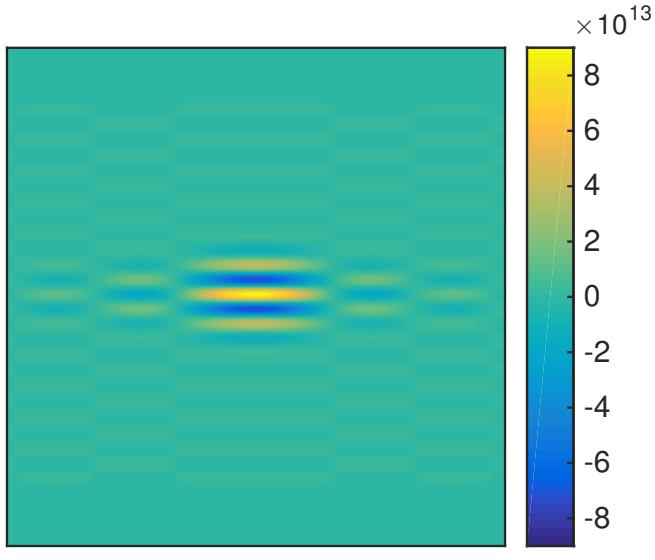

The real part of the PSF $\tilde{g}_0$

(The size of the square is $2\,\mathrm{mm} \times 2\,\mathrm{mm}$, and the horizontal and vertical axes are the x and z axes.)

Angle compounding

- In order to improve the decay in the x direction, (Montaldo et al., 2009) introduced angle compounding:

$$s^{\mathrm{ac}}_{\Theta}(\mathbf{x}) = \frac{1}{2\Theta}\int_{-\Theta}^{\Theta} s_\theta(\mathbf{x})\,d\theta, \qquad g^{\mathrm{ac}}_{\Theta}(\mathbf{x}) = \frac{1}{2\Theta}\int_{-\Theta}^{\Theta} \tilde{g}_\theta(\mathbf{x})\,d\theta$$

- A simple derivation shows that the PSF is

$$g^{\mathrm{ac}}_{\Theta}(\mathbf{x}) = \tilde{g}_0(\mathbf{x})\,\mathrm{sinc}(2\pi\nu_0 c_0^{-1}\Theta x)$$

- $\Theta = 0$: we recover $\tilde{g}_\theta$ for $\theta = 0$.
- $\Theta > 0$: this PSF enjoys faster decay in the variable x.

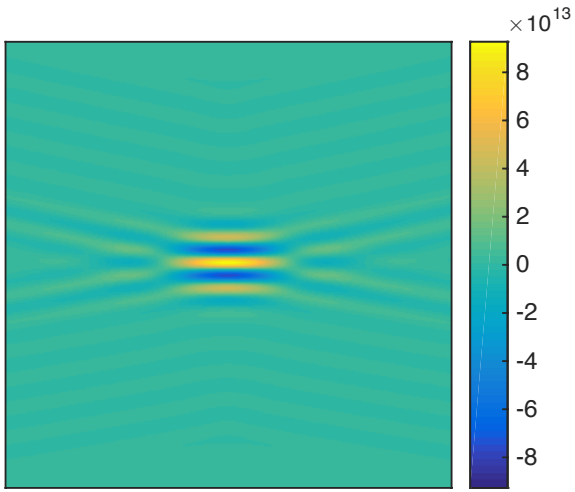

(a) g_θ, $\theta = 0$

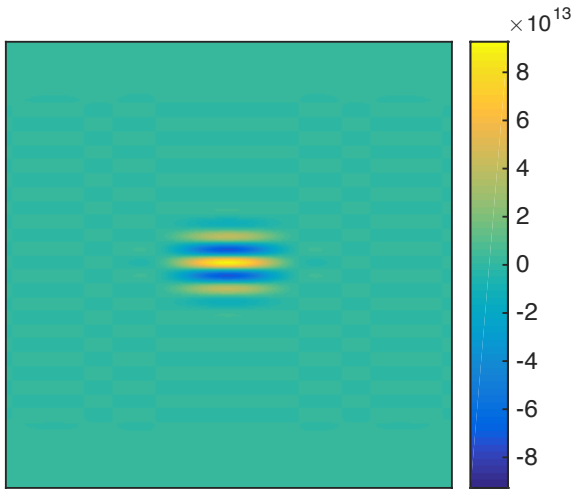

(b) g^{ac}_{Θ}, $\Theta = 0.25$

Angle compounding

- In order to improve the decay in the x direction, (Montaldo et al., 2009) introduced angle compounding:

$$s_\Theta^{\mathsf{ac}}(\mathbf{x}) = \frac{1}{2\Theta}\int_{-\Theta}^{\Theta} s_\theta(\mathbf{x})\,d\theta, \qquad g_\Theta^{\mathsf{ac}}(\mathbf{x}) = \frac{1}{2\Theta}\int_{-\Theta}^{\Theta} \tilde{g}_\theta(\mathbf{x})\,d\theta$$

- A simple derivation shows that the PSF is

$$g_\Theta^{\mathsf{ac}}(\mathbf{x}) = \tilde{g}_0(\mathbf{x})\,\mathrm{sinc}(2\pi\nu_0 c_0^{-1}\Theta x)$$

- $\Theta = 0$: we recover $\tilde{g}_\theta$ for $\theta = 0$.
- $\Theta > 0$: this PSF enjoys faster decay in the variable x.

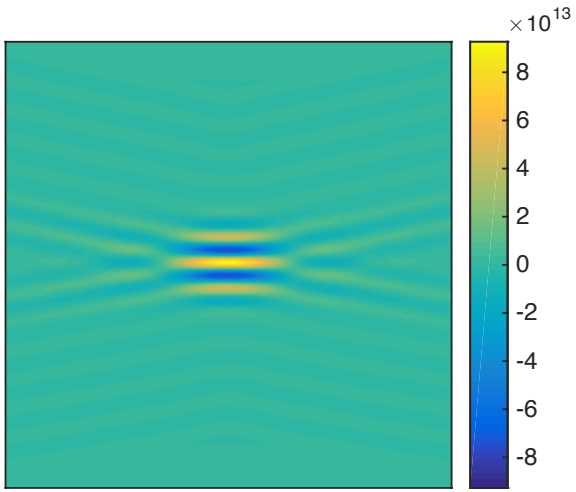

(c) g_θ, $\theta = 0$

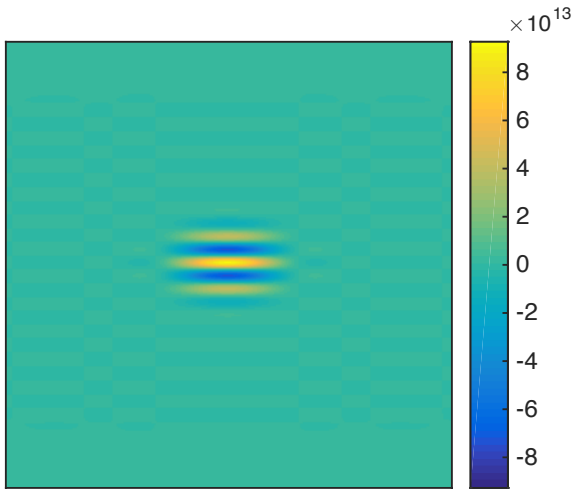

(d) g_Θ^{ac}, $\Theta = 0.25$

The dynamic forward problem

- The dynamic imaging setup consists in the repetition of the static imaging method over time to acquire a collection of images of a medium in motion.
- Quasistatic model: the whole process of obtaining one image is fast enough to consider the medium static, but collecting several images over time gives us a movie of the movement over time.
- There are two time scales: the fast one related to the propagation of the wave is considered instantaneous with respect to the slow one, related to the sequence of the images.
- We now neglect the time of the propagation of a single wave to obtain static imaging. The time t considered here is related to the slow time scale.
- At fixed time t, we obtain a static image of the medium $n = n(\mathbf{x}, t)$:

$$s(\mathbf{x}, t) = \left(g_{\Theta}^{\mathsf{ac}} * n(\,\cdot\,, t)\right)(\mathbf{x}).$$

The dynamic forward problem

- The dynamic imaging setup consists in the repetition of the static imaging method over time to acquire a collection of images of a medium in motion.
- Quasistatic model: the whole process of obtaining one image is fast enough to consider the medium static, but collecting several images over time gives us a movie of the movement over time.
- There are two time scales: the fast one related to the propagation of the wave is considered instantaneous with respect to the slow one, related to the sequence of the images.
- We now neglect the time of the propagation of a single wave to obtain static imaging. The time t considered here is related to the slow time scale.
- At fixed time t, we obtain a static image of the medium $n = n(\mathbf{x}, t)$:

$$s(\mathbf{x}, t) = \left(g_{\Theta}^{\mathsf{ac}} * n(\,\cdot\,, t)\right)(\mathbf{x}).$$

The dynamic forward problem

- The dynamic imaging setup consists in the repetition of the static imaging method over time to acquire a collection of images of a medium in motion.
- Quasistatic model: the whole process of obtaining one image is fast enough to consider the medium static, but collecting several images over time gives us a movie of the movement over time.
- There are two time scales: the fast one related to the propagation of the wave is considered instantaneous with respect to the slow one, related to the sequence of the images.
- We now neglect the time of the propagation of a single wave to obtain static imaging. The time t considered here is related to the slow time scale.
- At fixed time t, we obtain a static image of the medium $n = n(\mathbf{x}, t)$:

$$s(\mathbf{x}, t) = \left(g_{\Theta}^{\mathsf{ac}} * n(\,\cdot\,, t)\right)(\mathbf{x}).$$

The dynamic forward problem

- The dynamic imaging setup consists in the repetition of the static imaging method over time to acquire a collection of images of a medium in motion.
- Quasistatic model: the whole process of obtaining one image is fast enough to consider the medium static, but collecting several images over time gives us a movie of the movement over time.
- There are two time scales: the fast one related to the propagation of the wave is considered instantaneous with respect to the slow one, related to the sequence of the images.
- We now neglect the time of the propagation of a single wave to obtain static imaging. The time t considered here is related to the slow time scale.
- At fixed time t, we obtain a static image of the medium $n = n(\mathbf{x}, t)$:

$$s(\mathbf{x}, t) = \left(g_{\Theta}^{\mathsf{ac}} * n(\,\cdot\,, t)\right)(\mathbf{x}).$$

The dynamic inverse problem: Source separation

- Repeating the process for $t \in [0, T]$ we obtain the movie $s(\mathbf{x}, t)$, which represents the main data we now need to process.
- Main aim: locating the (possibly very small) blood vessels.
- Main issue: $s(x, t)$ is highly corrupted by clutter signal, namely, the signal scattered from tissues.
- Decompose

$$n(\mathbf{x}, t) = n_c(\mathbf{x}, t) + n_b(\mathbf{x}, t)$$

- The measurements are

$$s(\mathbf{x}, t) = s_c(\mathbf{x}, t) + s_b(\mathbf{x}, t)$$

- Inverse problem: determine the spatial support of n_b.

A general multiple scatterer random model

- Consider N point particles, with positions

$$a_k(t), \qquad k = 1, \dots, N.$$

- a_k: i.i.d. stochastic processes
- The medium and the measurements are given by

$$n(\mathbf{x}, t) = \frac{C}{\sqrt{N}} \sum_{k=1}^{N} \delta_{a_k(t)}(\mathbf{x}), \qquad s(\mathbf{x}, t) = \frac{C}{\sqrt{N}} \sum_{k=1}^{N} g(\mathbf{x} - a_k(t))$$

  - $C > 0$: scattering intensity
  - $\frac{1}{\sqrt{N}}$: natural normalization factor (central limit theorem)
- $(\mathbf{x}_i)_{i=1,\dots,m_{\mathbf{x}}}$, $(t_j)_{j=1,\dots,m_t}$: sampling locations and times.
- Casorati matrix $S_N \in \mathbb{C}^{m_{\mathbf{x}} \times m_t}$:

$$S_N(i, j) = s(\mathbf{x}_i, t_j).$$

- Multivariate central limit theorem: S_N converges in distribution to a Gaussian complex matrix $S \in \mathbb{C}^{m_{\mathbf{x}} \times m_t}$
- The distribution of S is entirely determined by g and the law of a_k

A general multiple scatterer random model

- Consider N point particles, with positions

$$a_k(t), \qquad k = 1, \dots, N.$$

- a_k: i.i.d. stochastic processes
- The medium and the measurements are given by

$$n(\mathbf{x}, t) = \frac{C}{\sqrt{N}} \sum_{k=1}^{N} \delta_{a_k(t)}(\mathbf{x}), \qquad s(\mathbf{x}, t) = \frac{C}{\sqrt{N}} \sum_{k=1}^{N} g(\mathbf{x} - a_k(t))$$

  - $C > 0$: scattering intensity
  - $\frac{1}{\sqrt{N}}$: natural normalization factor (central limit theorem)

- $(\mathbf{x}_i)_{i=1,\dots,m_{\mathbf{x}}}$, $(t_j)_{j=1,\dots,m_t}$: sampling locations and times.
- Casorati matrix $S_N \in \mathbb{C}^{m_{\mathbf{x}} \times m_t}$:

$$S_N(i, j) = s(\mathbf{x}_i, t_j).$$

- Multivariate central limit theorem: S_N converges in distribution to a Gaussian complex matrix $S \in \mathbb{C}^{m_{\mathbf{x}} \times m_t}$
- The distribution of S is entirely determined by g and the law of a_k

A general multiple scatterer random model

- Consider N point particles, with positions

$$a_k(t), \qquad k = 1, \dots, N.$$

- a_k: i.i.d. stochastic processes
- The medium and the measurements are given by

$$n(\mathbf{x}, t) = \frac{C}{\sqrt{N}} \sum_{k=1}^{N} \delta_{a_k(t)}(\mathbf{x}), \qquad s(\mathbf{x}, t) = \frac{C}{\sqrt{N}} \sum_{k=1}^{N} g(\mathbf{x} - a_k(t))$$

  - $C > 0$: scattering intensity
  - $\frac{1}{\sqrt{N}}$: natural normalization factor (central limit theorem)
- $(\mathbf{x}_i)_{i=1,\dots,m_{\mathbf{x}}}$, $(t_j)_{j=1,\dots,m_t}$: sampling locations and times.
- Casorati matrix $S_N \in \mathbb{C}^{m_{\mathbf{x}} \times m_t}$:

$$S_N(i, j) = s(\mathbf{x}_i, t_j).$$

- Multivariate central limit theorem: S_N converges in distribution to a Gaussian complex matrix $S \in \mathbb{C}^{m_{\mathbf{x}} \times m_t}$
- The distribution of S is entirely determined by g and the law of a_k

A general multiple scatterer random model

- Consider N point particles, with positions

$$a_k(t), \qquad k = 1, \dots, N.$$

- a_k: i.i.d. stochastic processes
- The medium and the measurements are given by

$$n(\mathbf{x}, t) = \frac{C}{\sqrt{N}} \sum_{k=1}^{N} \delta_{a_k(t)}(\mathbf{x}), \qquad s(\mathbf{x}, t) = \frac{C}{\sqrt{N}} \sum_{k=1}^{N} g(\mathbf{x} - a_k(t))$$

  - $C > 0$: scattering intensity
  - $\frac{1}{\sqrt{N}}$: natural normalization factor (central limit theorem)
- $(\mathbf{x}_i)_{i=1,\dots,m_{\mathbf{x}}}$, $(t_j)_{j=1,\dots,m_t}$: sampling locations and times.
- Casorati matrix $S_N \in \mathbb{C}^{m_{\mathbf{x}} \times m_t}$:

$$S_N(i, j) = s(\mathbf{x}_i, t_j).$$

- Multivariate central limit theorem: S_N converges in distribution to a Gaussian complex matrix $S \in \mathbb{C}^{m_{\mathbf{x}} \times m_t}$
- The distribution of S is entirely determined by g and the law of a_k

The SVD separation algorithm (Demené et al., 2015)

- Casorati matrix $S \in \mathbb{C}^{m_{\mathbf{x}} \times m_t}$ $(m_t \leq m_{\mathbf{x}})$:

$$S(i,j) = s(\mathbf{x}_i, t_j).$$

- The singular value decomposition of S

$$S(i,j) = \sum_{k=1}^{m_t} \sigma_k u_k(i) \bar{v}_k(j)$$

  - singular vectors: $(u_1, ..., u_{m_{\mathbf{x}}})$ and $(v_1, ..., v_{m_t})$ are ONB of $\mathbb{C}^{m_x}$ and $\mathbb{C}^{m_t}$
  - singular values: $\sigma_1 \geq \sigma_2 \geq ... \geq \sigma_{m_t} \geq 0$
  - the dynamic data S are expressed as a sum of spatial components u_k moving with time profiles v_k, with weights σ_k.

- Since the tissue movement has higher spatial coherence than the blood flow, the first factors are expected to contain the clutter signal, and the remainder to provide information about the blood location
- The blood location may be recovered by looking at the "power Doppler"

$$\hat{S}_{b,K}(i) := \sum_{k=K+1}^{m_t} \sigma_k^2 |u_k|^2(i), \qquad i \in \{1, ..., m_{\mathbf{x}}\}.$$

The SVD separation algorithm (Demené et al., 2015)

- Casorati matrix $S \in \mathbb{C}^{m_{\mathbf{x}} \times m_t}$ $(m_t \leq m_{\mathbf{x}})$:

$$S(i,j) = s(\mathbf{x}_i, t_j).$$

- The singular value decomposition of S

$$S(i,j) = \sum_{k=1}^{m_t} \sigma_k u_k(i) \bar{v}_k(j)$$

  - singular vectors: $(u_1, ..., u_{m_{\mathbf{x}}})$ and $(v_1, ..., v_{m_t})$ are ONB of $\mathbb{C}^{m_x}$ and $\mathbb{C}^{m_t}$
  - singular values: $\sigma_1 \geq \sigma_2 \geq ... \geq \sigma_{m_t} \geq 0$
  - the dynamic data S are expressed as a sum of spatial components u_k moving with time profiles v_k, with weights σ_k.

- Since the tissue movement has higher spatial coherence than the blood flow, the first factors are expected to contain the clutter signal, and the remainder to provide information about the blood location
- The blood location may be recovered by looking at the "power Doppler"

$$\hat{S}_{b,K}(i) := \sum_{k=K+1}^{m_t} \sigma_k^2 |u_k|^2(i), \qquad i \in \{1, ..., m_{\mathbf{x}}\}.$$

The SVD separation algorithm (Demené et al., 2015)

- Casorati matrix $S \in \mathbb{C}^{m_{\mathbf{x}} \times m_t}$ $(m_t \leq m_{\mathbf{x}})$:

$$S(i,j) = s(\mathbf{x}_i, t_j).$$

- The singular value decomposition of S

$$S(i,j) = \sum_{k=1}^{m_t} \sigma_k u_k(i) \bar{v}_k(j)$$

  - singular vectors: $(u_1, ..., u_{m_{\mathbf{x}}})$ and $(v_1, ..., v_{m_t})$ are ONB of $\mathbb{C}^{m_x}$ and $\mathbb{C}^{m_t}$
  - singular values: $\sigma_1 \geq \sigma_2 \geq ... \geq \sigma_{m_t} \geq 0$
  - the dynamic data S are expressed as a sum of spatial components u_k moving with time profiles v_k, with weights σ_k.

- Since the tissue movement has higher spatial coherence than the blood flow, the first factors are expected to contain the clutter signal, and the remainder to provide information about the blood location
- The blood location may be recovered by looking at the "power Doppler"

$$\hat{S}_{b,K}(i) := \sum_{k=K+1}^{m_t} \sigma_k^2 |u_k|^2(i), \qquad i \in \{1, ..., m_{\mathbf{x}}\}.$$

Justification of the SVD method (1D)

- Using the multiple scatterer random model introduced above, we construct two Casorati matrices

$$S_b,\ S_c$$

as limits of particles with the following statistics.

- Clutter: large support, constant velocities

$$a_k(t) = u_k + v_c t$$

where u_k is uniformly distributed in $(0, L_c)$.

- Blood: small support, varying velocities:

$$a_k(t) = u_k + v_b t + \sigma B_t$$

where u_k is uniformly distributed in $(0, L_b)$ $(L_b \ll L_c)$ and B_t is a Brownian motion.

- S_b and S_c may be constructed using the Gaussian limit approximation

Justification of the SVD method (1D)

- Using the multiple scatterer random model introduced above, we construct two Casorati matrices

$$S_b,\ S_c$$

as limits of particles with the following statistics.

- Clutter: large support, constant velocities

$$a_k(t) = u_k + v_c t$$

where u_k is uniformly distributed in $(0, L_c)$.

- Blood: small support, varying velocities:

$$a_k(t) = u_k + v_b t + \sigma B_t$$

where u_k is uniformly distributed in $(0, L_b)$ $(L_b \ll L_c)$ and B_t is a Brownian motion.

- S_b and S_c may be constructed using the Gaussian limit approximation

Justification of the SVD method (1D)

- Using the multiple scatterer random model introduced above, we construct two Casorati matrices

$$S_b,\ S_c$$

as limits of particles with the following statistics.

- Clutter: large support, constant velocities

$$a_k(t) = u_k + v_c t$$

where u_k is uniformly distributed in $(0, L_c)$.

- Blood: small support, varying velocities:

$$a_k(t) = u_k + v_b t + \sigma B_t$$

where u_k is uniformly distributed in $(0, L_b)$ $(L_b \ll L_c)$ and B_t is a Brownian motion.

- S_b and S_c may be constructed using the Gaussian limit approximation

Justification of the SVD method (1D)

- Using the multiple scatterer random model introduced above, we construct two Casorati matrices

$$S_b,\ S_c$$

as limits of particles with the following statistics.

- Clutter: large support, constant velocities

$$a_k(t) = u_k + v_c t$$

where u_k is uniformly distributed in $(0, L_c)$.

- Blood: small support, varying velocities:

$$a_k(t) = u_k + v_b t + \sigma B_t$$

where u_k is uniformly distributed in $(0, L_b)$ $(L_b \ll L_c)$ and B_t is a Brownian motion.

- S_b and S_c may be constructed using the Gaussian limit approximation

Justification of the SVD method (1D)

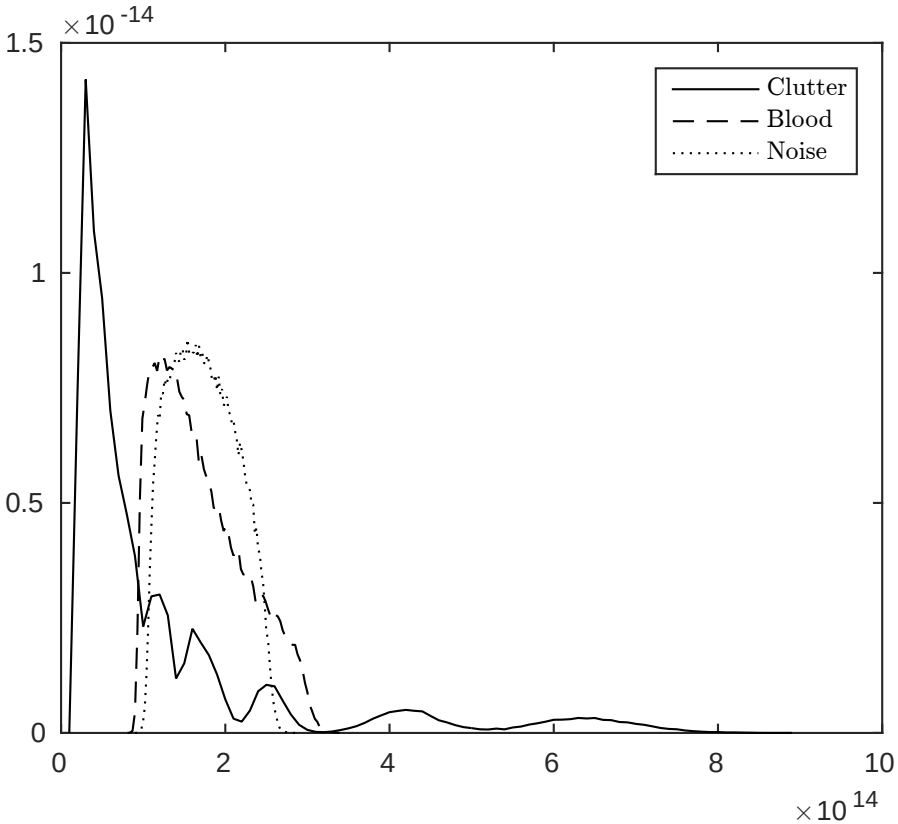

(a) The clutter model ($v_c = 10^{-2}\,\mathrm{m{\cdot}s^{-1}}$), the blood model ($\sigma^2 = 10^{-6}\,\mathrm{m^2 s^{-1}}$, $v_b = 10^{-2}\,\mathrm{m{\cdot}s^{-1}}$) and a white noise model with same variance as the blood.

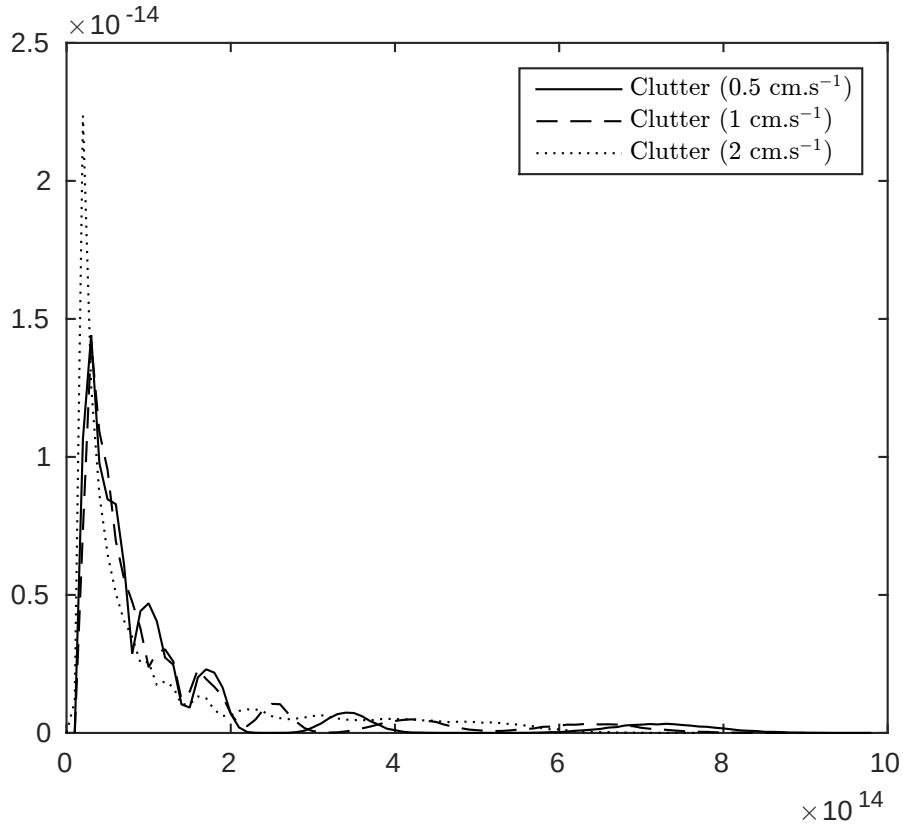

(b) The clutter model with different velocities.

Figure: The distribution of the singular values of the Casorati matrix S in different cases.

Numerical simulations

We put one blood vessel in a moving tissue:

- domain: $5\,\mathrm{mm} \times 5\,\mathrm{mm}$
- $F = 0.4$ and $\Theta = 7°$.
- The density of particles for both blood and clutter is 2,000 per mm^2
- $C_c = 5C_b$

A single frame of the measurements $s(\mathbf{x}, t_0)$ is

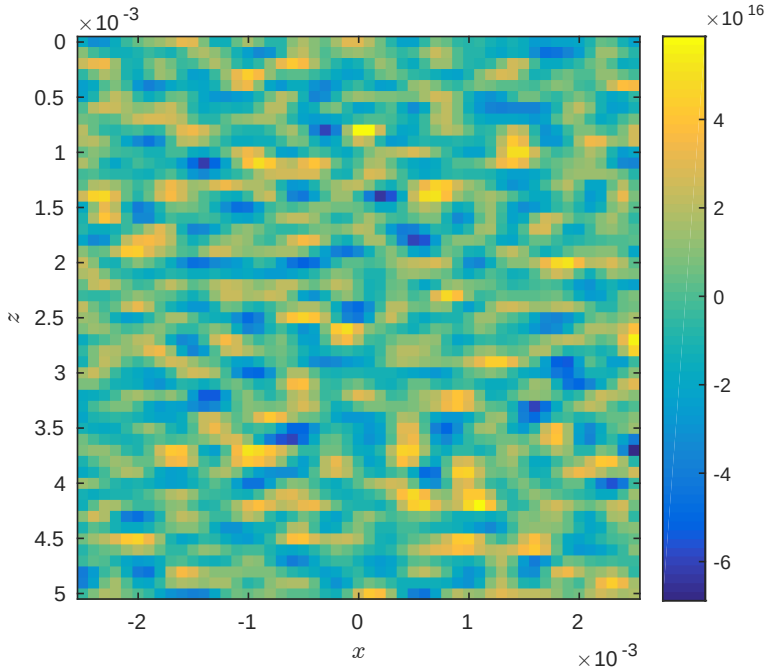

Need further processing to locate the blood vessel!

Numerical simulations: $v_b > v_c$

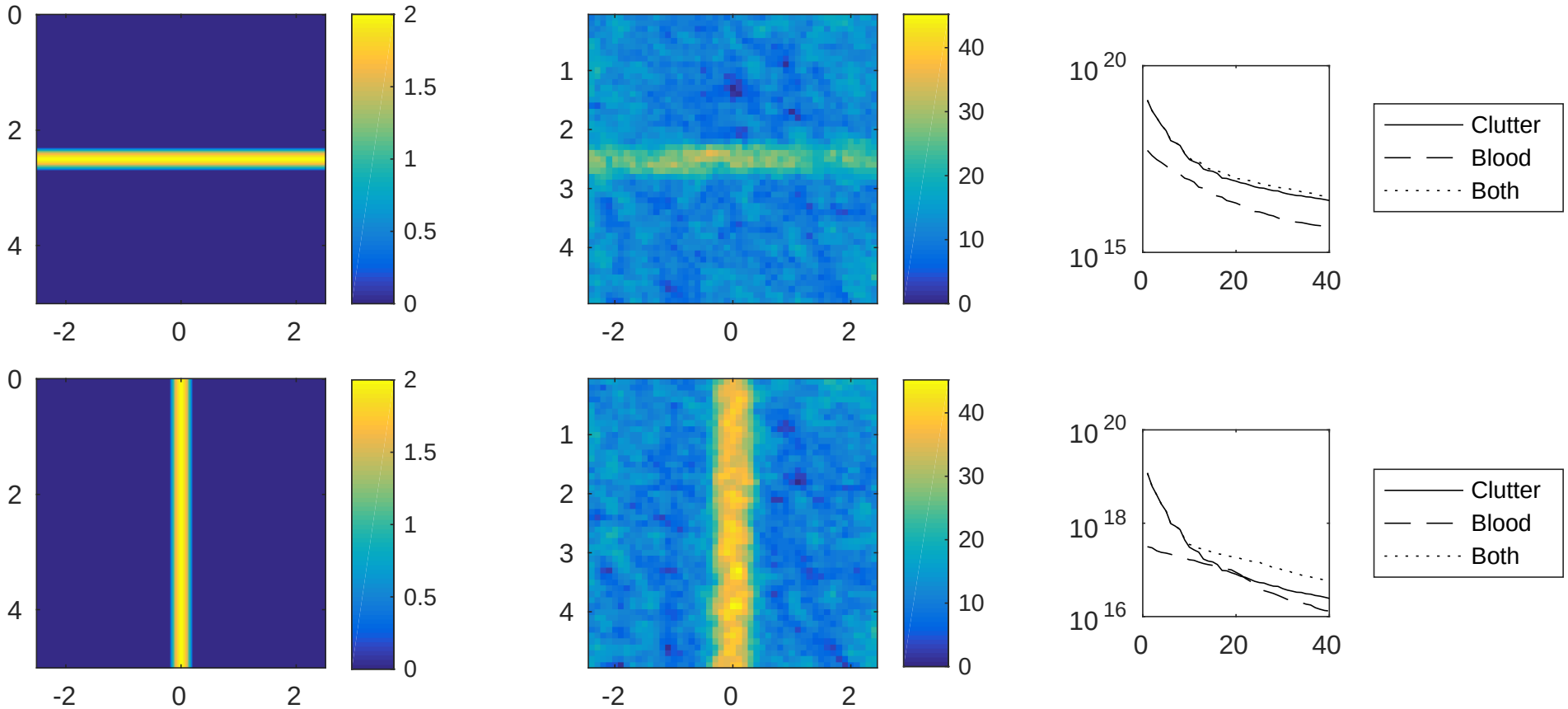

(a) Maximum blood velocity: $2\,\mathrm{cm\cdot s^{-1}}$; mean clutter velocity: $1\,\mathrm{cm\cdot s^{-1}}$.

Numerical simulations: $v_b = v_c$

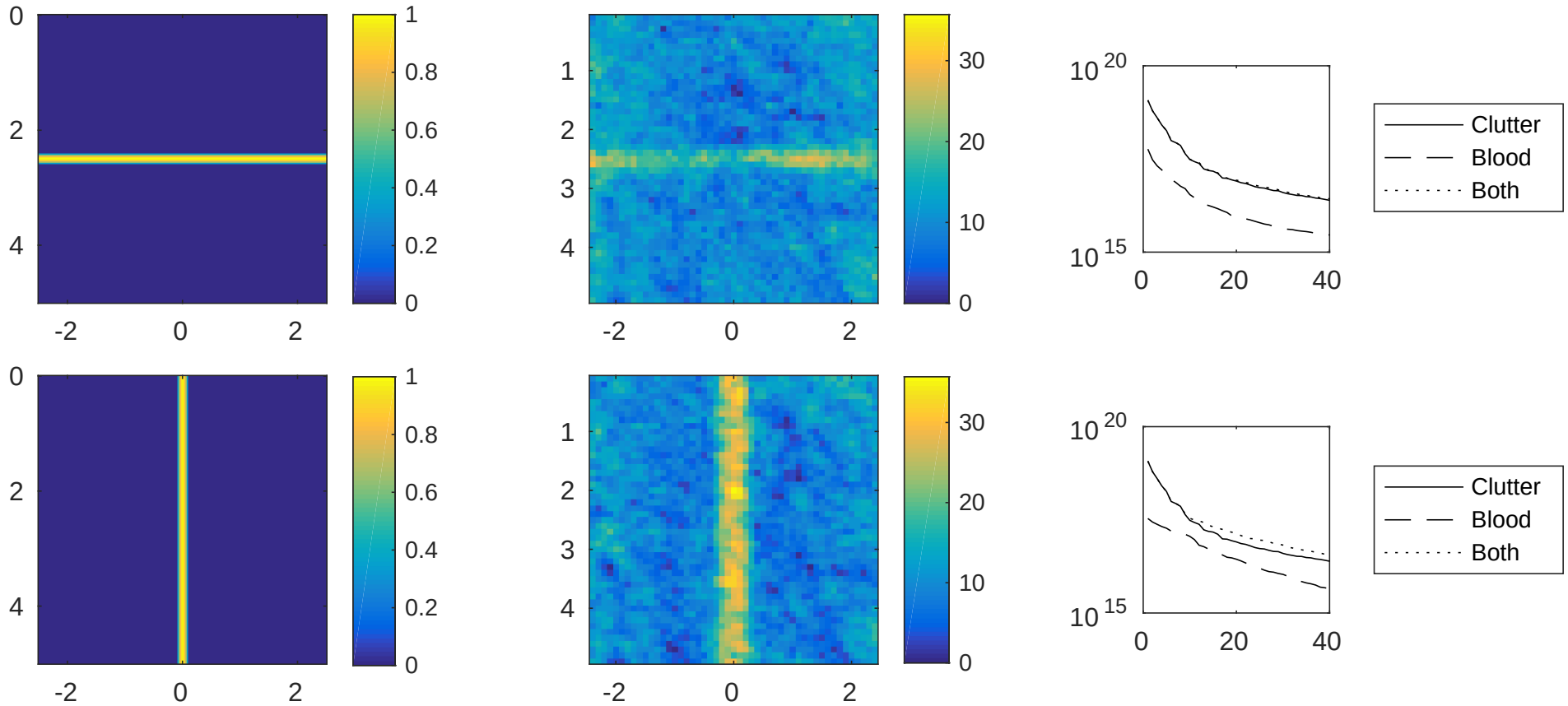

(b) Maximum blood velocity: $1\,\mathrm{cm{\cdot}s^{-1}}$; mean clutter velocity: $1\,\mathrm{cm{\cdot}s^{-1}}$.

Numerical simulations: $v_b < v_c$

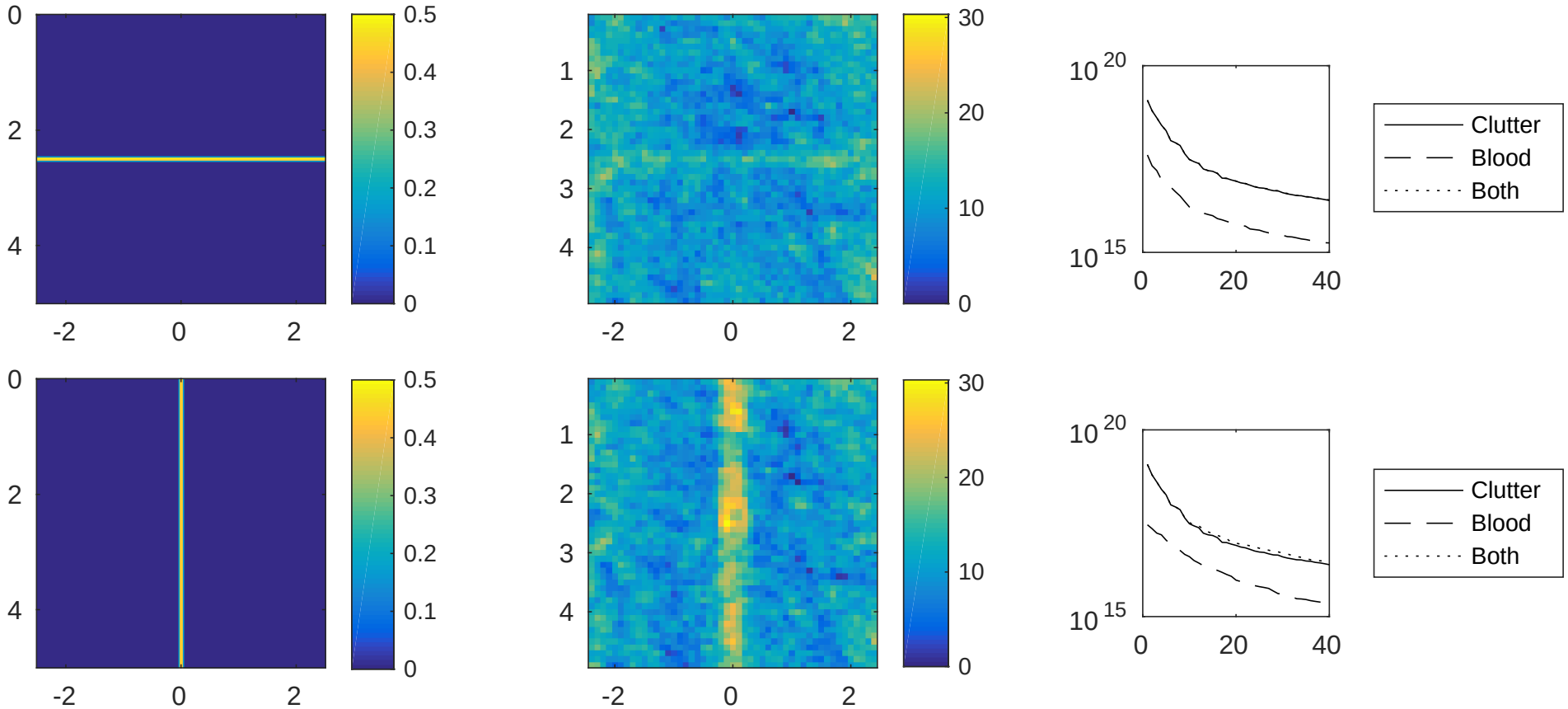

(c) Maximum blood velocity: $0.5\,\mathrm{cm\cdot s^{-1}}$; mean clutter velocity: $1\,\mathrm{cm\cdot s^{-1}}$.

Numerical simulations: the flow direction

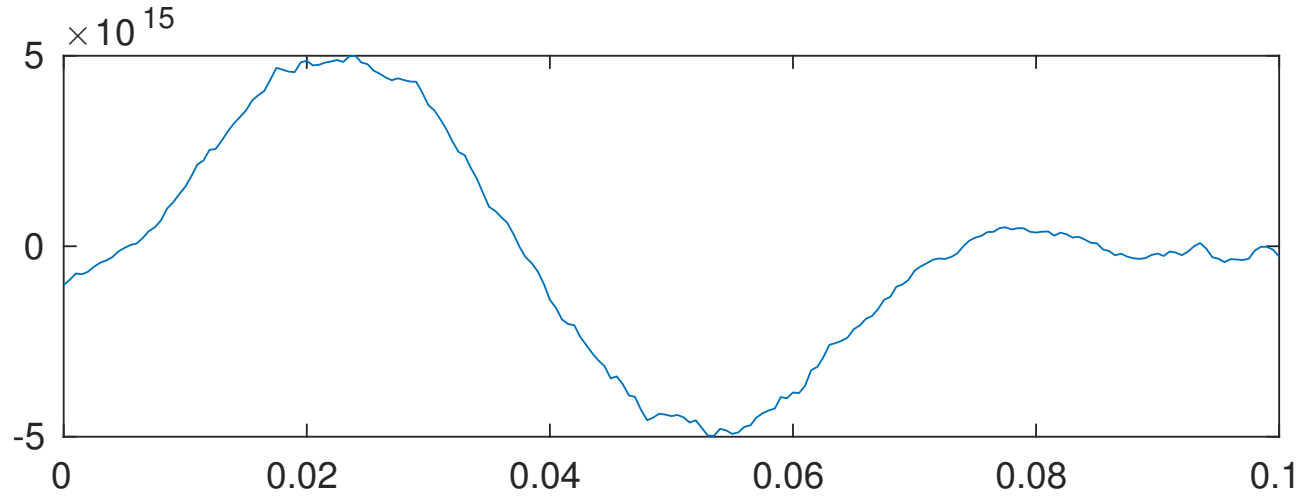

(a) Flow parallel to the receptor array.

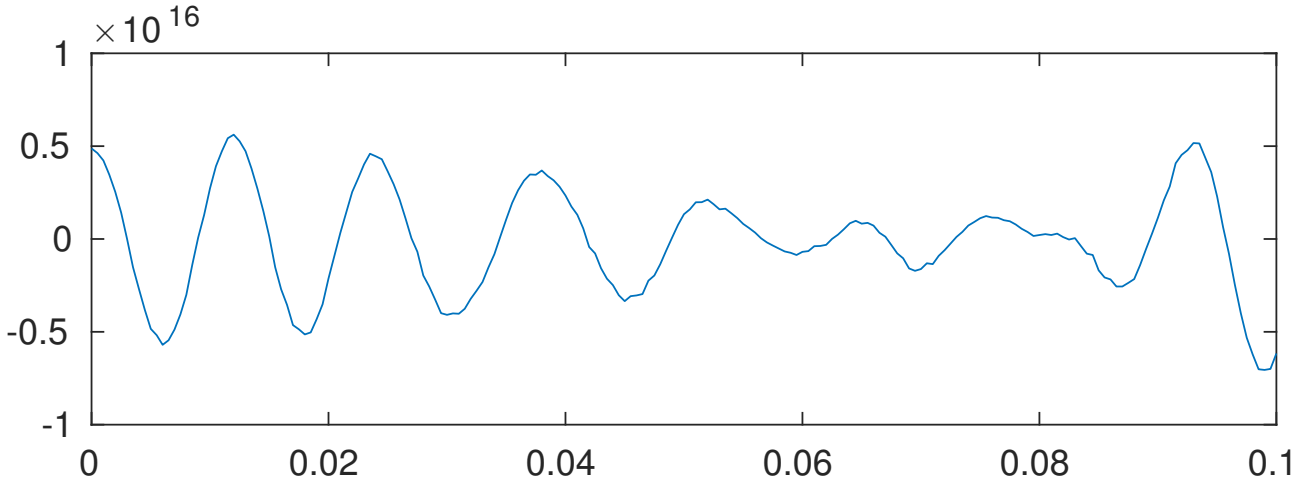

(b) Flow perpendicular to the receptor array.

Figure: Time behavior of a single pixel (real part), located in a constant velocity flow.

Numerical simulations: robustness to noise

- Independent white Gaussian noise
- contrast: ratio between the mean intensity of the reconstructed image inside and outside the blood domain.
- $C_c = 5C_b$: a noise intensity of 10% corresponds to half the intensity of blood

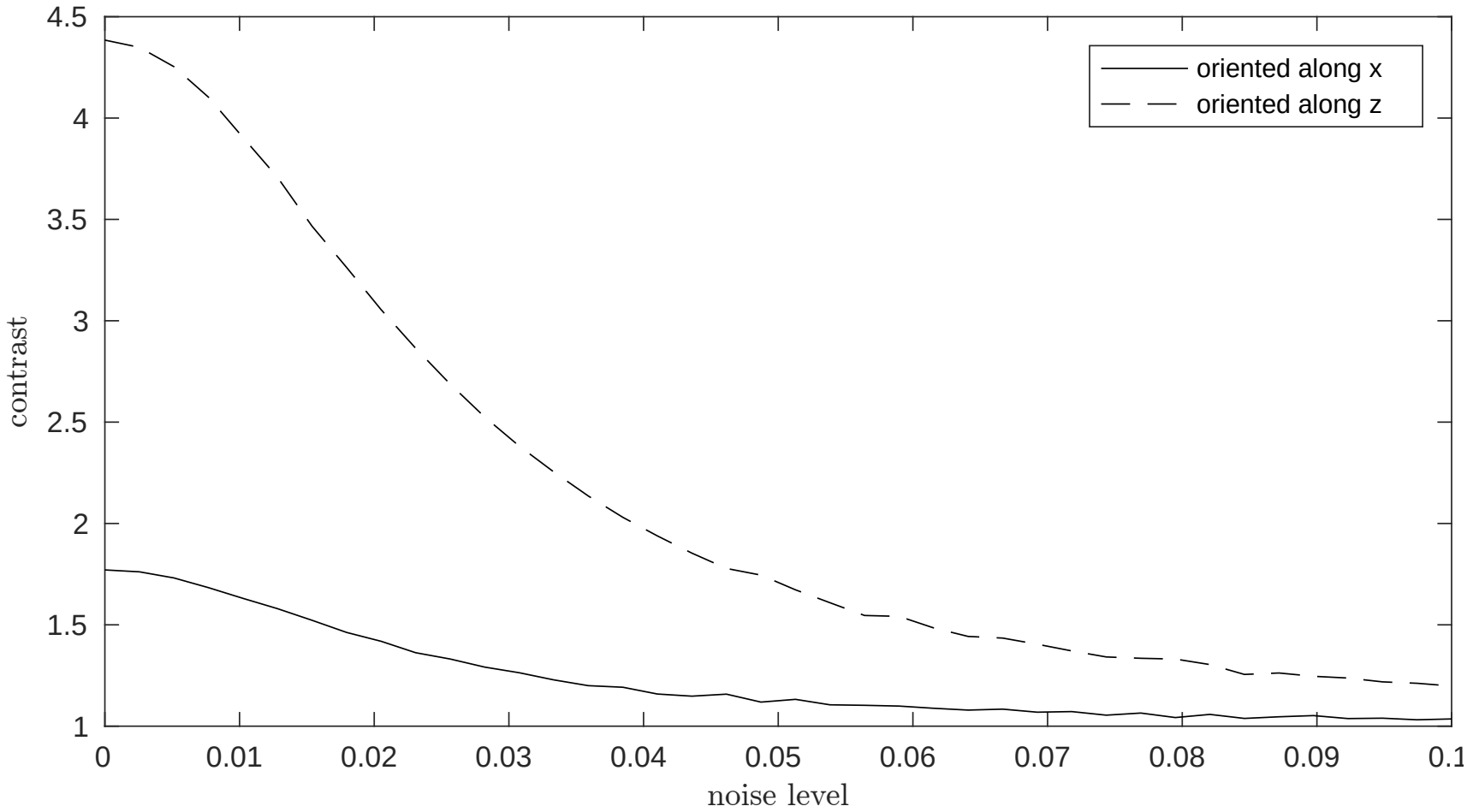

Superresolution with ultrafast ultrasound

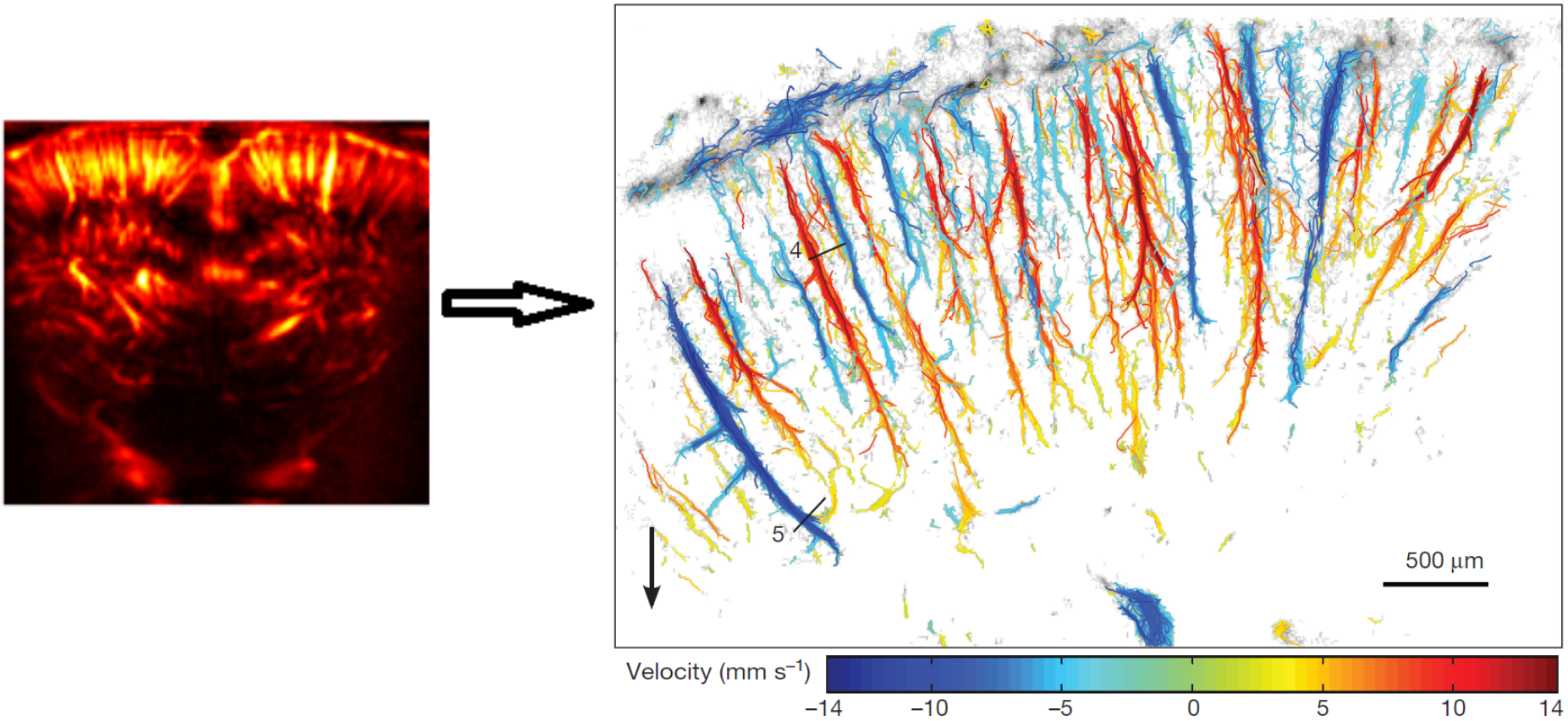

Errico et. al, Nature 527, 499–502, 2015

Superresolution: ongoing work

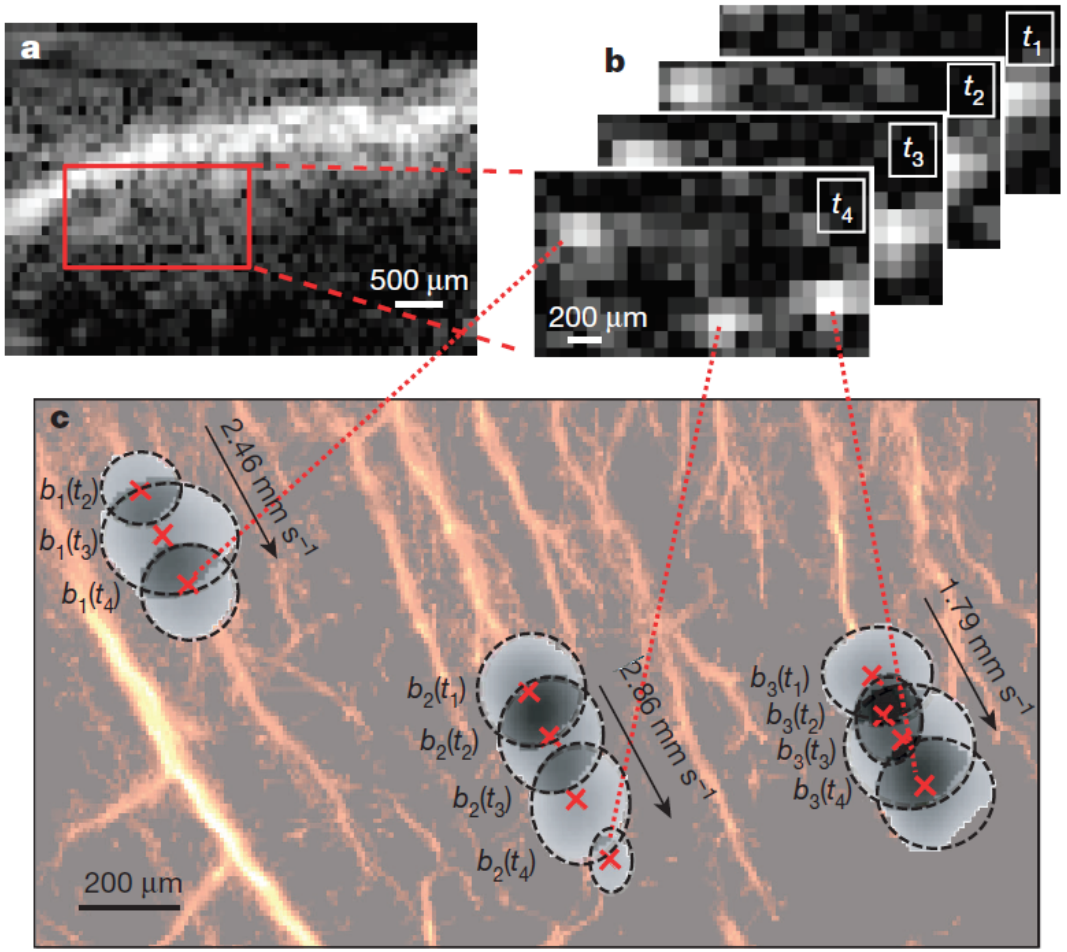

Errico et. al, Nature 527, 499–502, 2015

Current method

- $\mathbf{a} \to \mathbf{b}$: SVD
- $\mathbf{b} \to \mathbf{c}$: identify center of PSF, if well-separated
- Track bubbles to obtain velocities
- Drawbacks:
  - slow
  - discard a lot of data

New method

- dynamic superresolution in time and space
- based on ℓ^1 minimization
- obtain locations and velocities in one step

Superresolution: ongoing work

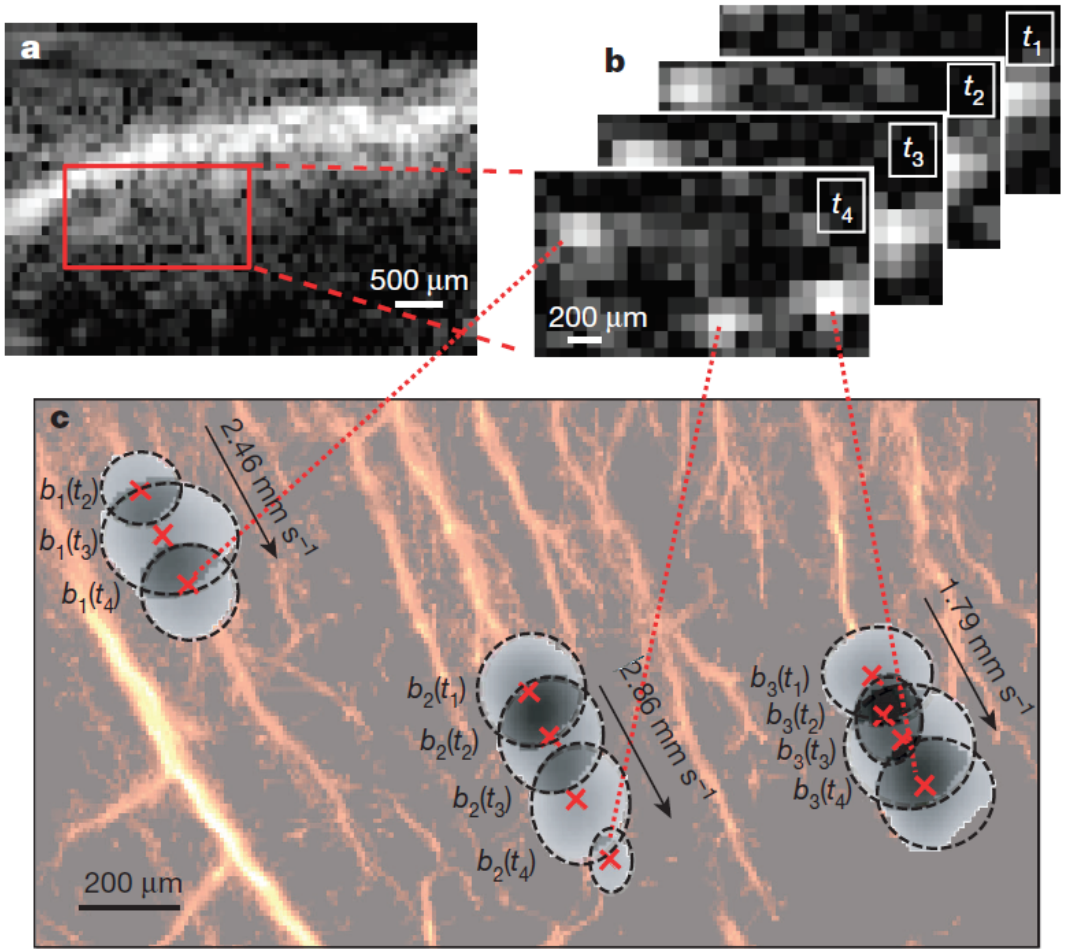

Errico et. al, Nature 527, 499–502, 2015

Current method

- $\mathbf{a} \to \mathbf{b}$: SVD
- $\mathbf{b} \to \mathbf{c}$: identify center of PSF, if well-separated
- Track bubbles to obtain velocities
- Drawbacks:
  - slow
  - discard a lot of data

New method

- dynamic superresolution in time and space
- based on ℓ^1 minimization
- obtain locations and velocities in one step